Indian Journal of Pure & Applied Physics
Vol. 61, June 2023, pp. 520-525
DOI: 10.56042/ijpap.v61i6.2435

Assessment of Radionuclide Concentration and Exhalation Rates in some NORMs and TENORMs of Shivalik Region

Jaswinder Kaur[a,b], Deep Shikha[c], Vimal Mehta[c*] & R P Chauhan[d]

[a]Department of Physics, Punjabi University, Patiala 147 002, India

[b]Department of Applied Sciences, Chandigarh Group of Colleges, Jhanjeri, Mohali 140 307, India

[c]Department of Physics, Sri Guru Teg Bahadur Khalsa College, Sri Anandpur Sahib 140 118, India

[d]National Institute of Technology, Kurukshetra 136 119, India

Received 20 February 2023; accepted 23 May 2023

^{226}Ra, ^{232}Th, their decay products ^{222}Rn, ^{220}Rn and ^{40}K significantly contribute to the mean dose from natural background radiation. This study reports the concentration of radionuclides in Naturally Occurring Radioactive Materials (NORMS) and Technologically Enhanced Naturally Occurring Radioactive Materials (TENORMS) of the Shivalik region of Punjab and Himachal Pradesh. The activity of radionuclides ^{226}Ra, ^{232}Th and ^{40}K in different NORMS (soil, sand, rocks) and TENORMS (tiles, marble, cement) were calculated by Gamma spectrometry method using an HPGe detector. Radon mass exhalation and thoron surface exhalation rates were also determined using a Smart RnDuo monitor for the above samples. From the results, it could be concluded that the radon mass exhalation rate and radium activity were obtained to be maximum for tile no. 2 and minimum for white marble samples. Similarly, the thoron surface exhalation rate and thorium activity occurred maximum in tile no. 2 and minimum for safedi. The radium equivalent activity (Ra_{eq}), gamma activity concentration index (I), internal hazard index (H_{int}) and external hazard index (H_{ext}) were computed using appropriate relations. The values range between 5.858 to 188.944, 0.0403 to 1.377, 0.028 to 0.615 and 0.015 to 0.510 having mean values of 107.256, 0.685, 0.325, and 0.256, respectively.

Keywords: Dose, Gamma spectrometry, Exhalation, Smart RnDuo, hazard index

Introduction

NORMS are present all over the earth's map. This term is used to characterize minerals and other materials, including radionuclides from natural roots, which become a reason for remarkable growth in exposure to employees or people and cannot be ignored from the radiation safety point of view. ^{238}U, ^{232}Th and ^{40}K are the three main long-lived radioactive materials in NORM present in the earth's crust. Humans are continuously exposed to this natural radiation every day. Artificial sources ^{137}Cs also cause radiation exposure. Due to human actions like energy-yielding, mining, industrial waste, and military functioning like nuclear accidents or weapon examination, these radionuclides may be released into the environment[1]. These radionuclides pose a potential hazard to human wellness due to the ejection of ionizing radiation[2]. Another activity, like flying at high altitudes, also increases natural exposure to the ahead limit. Controlling people's exposure to background radiation necessitates learning more about the classification, characteristics and levels of radionuclides found in rocks and soils. TENORMS include wastes with a small specific activity liberated from the various manufacturing projects, including uranium mining, production of phosphate fertilizers, chemical processing of ores, removal, and cleansing of trace elements, *etc*. In TENORMS, Radionuclides ^{238}U, ^{232}Th and their respective disintegrate products are present in the majority. Other radionuclides ^{40}K, ^{87}Rb and ^{137}Cs are present in levels of background doses.

It is well-known that the distribution of radiation over the globe is not uniform but varies according to factors like the abundance of radioactive elements in the planet's crust[3]. The level of radionuclides in plants is linearly linked to radionuclide concentration in soil[4], and it can be further increased by applying phosphate fertilizers which contains radioactivity almost ten times higher than the mean concentration of soil. The manufacturing, shipping, storing and usage of these fertilizers become the causes of increased doses of exposure to humans[5]. The samples of TENORMS are building materials like gypsum,

*Corresponding author: (E-mail: vimal78mehta@gmail.com)

granite, marble, cement, different types of wall colors, white cement, etc. These construction materials may also cause increase radioactivity significantly in radiation doses.

Radon and thoron are substantial donors to radiations' mean natural background dose. They correspond to around half of the total dose received from entirely natural sources of ionizing radiation[6]. These radioisotopes enter into the environment through two processes known as emanation and exhalation. Firstly, escape from the grains forming the medium, a process named emanation, then from the medium's top is called exhalation[7]. The entry of ^{222}Rn into the indoor environment happens predominantly due to the exhalation of ^{222}Rn from the soil and construction materials. These factors depend upon other parameters like half-life, aggregation rate of these gases in the interior domain, microstructure of materials, diffusion, advection, absorption etc. The time at which half of the ^{222}Rn atoms decay is 3.8days while for ^{220}Rn is 55.6 sec. Because of this half-life inequality, the dose from thoron and its daughter products is much lesser than radon and its progeny, which is around 10% of the former[8]. Generally, indoor radon concentration is higher than the thoron indoor concentration. However, the latter becomes vital because of the significant accumulation rate of its progeny (^{212}Pb having a half-life of 10.6 h) in breathable air[9]. Some studies [10, 11] also show that ^{220}Rn concentrations are justifiably equivalent to ^{222}Rn and its progeny in a few areas of lifted radiation's threats.

Kaur[12] reviewed the activity concentration in the states of North India: Uttar Pradesh, Punjab, Rajasthan and Haryana. Out of which, a higher concentration of ^{232}Th was observed in some districts of Punjab. In contrast, a higher content of ^{226}Ra and ^{40}K was noticed in some districts of Haryana, which may be due to the excessive adoption of abundant potassium fertilizers for agricultural growth. Mehta[13] reports the radon mass exhalation rate of Mohali, Punjab which is found to be lower than the mean of the worldwide value 57 mBqKg^{-1}h^{-1}.Semwal[14] publish the exhalation report from Almora, Uttarakhand, India of soil and building materials. Variation of mass exhalation rate observed from 16 to 54 mBq.kg^{-1}h^{-1}, while the area exhalation rate lies between 0.65 and 6.43 Bq.m^{-2}.s^{-1}. Rani[15] reported the exhalation rate in soil samples of Barnala and Moga districts. The radon mass exhalation rates have been found to vary from 4.56 ± 0.53 to 41.13 ± 1.21 mBqkg^{-1} h^{-1} with an average value of 24.8 ± 1 mBqkg^{-1} h^{-1} while thoron surface exhalation rates lie in the range from 1.50 ± 0.63 to 23.77 ± 1.52 kBqm^{-2} h^{-1} with mean value of 15.62 ± 1.24 kBqm^{-2} h^{-1} . Kansal[16] reports the measurements of ^{226}Ra,^{232}Th and ^{40}K and exhalation rates in soil samples collected from some parts of western districts of Haryana, India. The activity concentrations of ^{226}Ra, ^{232}Th and ^{40}K range from 13.93 to 142 Bq kg^{-1}, 35.95 to 91.78 Bq kg^{-1} and 299.57 to 1056.77 Bq kg^{-1}, respectively. The radium equivalent activity (Ra_{eq}) in all the soil samples varies from 92.51 to 287.08 Bq kg^{-1} with an average of 184.15 Bq kg^{-1}.

Intake of these radionuclides gases and their progenies causes several health hazards. The inadequately ventilated areas result in high population exposure to these gases compared to other areas. Long-term exposure to these gases in houses, buildings and workplaces amplifies the hazard of Lung Cancer[17].

The present study measures the exhalation rate of ^{222}Rn and ^{220}Rn in NORMS (soil, sand, rocks etc.) and TENORMS (common building materials).

1 Study Area

1.1 Punjab

The Indo-Gangetic basin. The region's dominant economic feature is agriculture, which has consequently shaped the foundation of Punjabi culture, where an individual's social standing is often contingent on land ownership. The physiographic setting of the state is characterized by two primary geomorphic entities - the Siwalik foothills in the northeast and the alluvial fill of the Indus drainage basin. The geological units of the Punjab state consist of the Siwalik Supergroup and Quaternary alluvium. The latter includes older and newer alluvium, with a maximum sediment depth of 4500m. The Siwalik Supergroup is further classified into three groups - Lower, Middle, and Upper Siwalik groups. The fertile plains of Punjab are renowned for their high agricultural productivity, accounting for roughly two-thirds of India's annual food grain production. The region predominantly features calcareous soil, including soil and sierozem soil, with alluvial soil generally described as arid and brown. In eastern Punjab, the soil type ranges from loamy to clayey[18].

1.2 Himachal Pradesh

Himachal Pradesh is a state located in the northern part of India, positioned within the Western Himalayas. Being one of the thirteen mountain states,

it is renowned for its challenging terrain, featuring numerous peaks and vast river systems. The geology of Himachal Pradesh is primarily characterized by Precambrian rocks that were assembled and deformed during the collision between India and Asia, followed by the Himalayan orogeny. The state's elevation ranges from 320m to 6975m, with rock materials largely sourced from the Indian craton, and their ages ranging from the Paleoproterozoic era to the present day. It is generally agreed that the Indian craton collided with Asia around 50-60 million years ago, causing extensive thrusting and folding of rock sequences during the collision. The area has also undergone substantial orographic precipitation, glaciation, and rapid erosion, shaping its overall landscape. Himachal Pradesh's exposed geological formations range from the Proterozoic to the Quaternary period, representing a classic geological sequence. The undifferentiated Proterozoic rocks are predominantly confined to the Lesser Himalaya and are represented by the Jutogh and Vaikrita groups. The Jutogh Group comprises formations such as Panjerli, Manal, Bhotli, Khirki, Taradevi, Kanda, Naura, Badrol, Rohru, Chirgaon, and Jaknoti, consisting of a thick sequence of carbonaceous phyllite, quartzite, and slate[18].

2 Materials and Methodology

2.1 Sampling Procedure

The materials were categorized into two classes-NORMS and TENORMS. In the category of TENORMS, 15 samples of building materials such as gypsum, granite, limestone, bricks, marble, white cement, interlock tiles, cement and tiles were aggregated from various vendors. For the collection of NORMS, different types of soils, sand, and rocks of various sizes were assembled from the river named 'Sutluj' collected. The samples must be free from other impurities. The materials, like bricks, tiles, marbles etc. were in their original size. Firstly, they were broken using a heavy pestle into coarse parts. Afterwards, all the samples were grinded using a grinder and sieved through 100-micron mesh to keep the uniformity of the grains. The mass of each sample varied from 1.5 kg to 2 kg. The collected soil samples were appropriately labelled. The samples were kept in an oven to dry at 105˚C for 48 hours and sieved. Before the radiometric analysis, each sample was sealed in an air-tight Marinelli beaker to prohibit liberation of ^{222}Rn and ^{220}Rn from the samples and stored for four weeks to obtain equilibrium between ^{226}Ra, ^{232}Th and their decay products. To determine the rate of exhalation from each location, dried samples of mass approximately 1 kg were taken in a polyethylene bag.

2.2 Smart RnDuo Monitor

SMART RnDuo Monitor (Alpha-Scintillometer GBH2002 with Lucas cell), designed and calibrated by BARC (Bhabha Atomic Research Centre), Mumbai, India[19], is adopted for the quantification of ^{222}Rnmass exhalation (J_{rm}) and ^{222}Rn areal exhalation (J_{ts}) rate in compiled samples. The ZnS:Ag screen works like a scintillation material having a volume of 150 cc. The principle is defined as the spotting of alpha radiations produced from radon decayand their progenies within the walls of detector volume detected by a scintillation screen coated alongside ZnS:Ag. The sensitivity factor of the monitor is 1.2 counts per hour (Bq.m^{-3}), and the detection limit lies between 8 Bq.m^{-3}and 10 MBq.m^{-3}.

A sample of known weight was placed into an exhalation chamber to measure J_{rm}. The experimental setup shown in Fig. 1 shows that measurement was done in diffusion mode and detector probe should be coupled with an exhalation chamber. The exhalation chamber consists of a cylindrical accumulator of stainless steel with an inner diameter of 30 cm and a height of 5 cm. The time cycle for measurement was 60 minutes, and a minimum of 18 cycles was required for measurement. The formula used for radon concentration C(t) at time T is[21]

$$C(t) = \frac{J_{rm}M}{V\lambda_r}\left(1 - e^{-\lambda_r T}\right) + C_0 e^{-\lambda_r T} \quad ...(1)$$

Where, C_0 is the radon concentration (Bq m^{-3}), M is the weight of the prepared sample (kg) placed in the chamber, λ_r is the effective radon decay constant, and T is the time (h) of measurement.

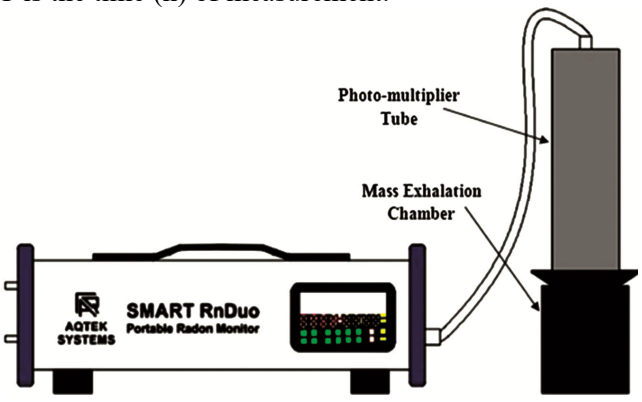

Fig. 1 — Experimental setup of Smart RnDuo for measurement of ^{222}Rn exhalation[20].

The sampling was done in flow mode for the measurement of J_{ts}, where two cylindrical pipes of diameter 0.5 cm were used through the chamber's top to function as the inlet and outlet of airflow for the determination of thoron concentration. The exhalation chamber is linked to the pump inlet of the monitor. A closed-circuit loop formed as the detection box was linked to the Smart RnDuo monitor via the airflow pump. Four cycles of time 15 min were used for analysis. Pump should be kept on for an initial 5 min to determine the background of the thoron. The J_{ts} ($Bqm^{-2}h^{-1}$) of thoron in closed loop[22] is given by Eq. (2):

$$J_{ts} = \frac{C_{eq} \times V \times \lambda}{A} \quad ...(2)$$

Where, C_{eq} ($Bq.m^{-3}$) accounts for the mean of observations of thoron gas concentration, V (m^3), is

Effective volume, λ is the decay constant (0.012464 s^{-1} for ^{222}Rn), and A is the sample's surface area (m^2).The measurement of every sample was done 2-3 times to increase the precision and accuracy found by the inventor of the instrument.

2.3 Gamma Spectrometric analysis

A 42% relative efficiency n-type low background HPGe coaxial cylindrical gamma spectrometer with a detector made by CANBERRA, USA, was used for radioactivity measurements. Lead was used as a shielding material with fixed bottom and a purity of 99.9%. The movable cover was used to reduce background radiation in the spectrum. The detector was linked with 16K MCA and ^{60}Co emission for data acquirement. The period of 50,000 sec was enough for data collection to yield better statistics. The net sample count rate was derived after subtracting the corresponding background rate at each energy peak. In the same way, an empty Marinelli beaker was also computed for the determination of background radiation. The calibration of energy and efficiency of the spectrometer was calculated by adopting Marinelli calibration sources, including ^{210}Pb, ^{241}Am, ^{109}Cd, ^{57}Co, ^{113}Sn, ^{85}Sr, ^{137}Cs

3 Results and Discussion

Table 1 shows that the activity concentrations of ^{226}Ra, ^{232}Th, and ^{40}K obtained from samples vary from 4.5±0.4 $Bq.kg^{-1}$ to 41.7±1.1 $Bq.kg^{-1}$, 0.1 $Bq.kg^{-1}$ to 89.75 $Bq.kg^{-1}$, and 1.4 $Bq.kg^{-1}$ to 508±11 $Bq.kg^{-1}$ respectively. These values lie within the range of radionuclides given by UNSCEAR (United Nations Scientific Committee on the Effects of Atomic Radiation) [22]. The values of the concentrations of radionuclides ^{226}Ra, ^{232}Th and ^{40}K and Radium equivalent activity (Ra_{ea}), Gamma activity concentration index (I), internal hazard index (H_{int}) and external hazard index (H_{ext}) are given in Table 1.

Table 1 — Activity of ^{226}Ra, ^{232}Th and ^{40}K in $Bq.kg^{-1}$, Ra_{ea}, I, H_{int} and H_{ext} for different samples

Sr. No.	Sample	^{226}Ra ($Bqkg^{-1}$)	^{232}Th ($Bqkg^{-1}$)	^{40}K ($Bqkg^{-1}$)	Ra_{ea}	I	H_{int}	H_{ext}
1	Tile 2	41.7±1.1	89.7±2.1	357.51±91	177.19	1.2713	0.591	0.478
2	Tile 3	15.4±0.8	68.2±2.7	319.74±19	142.546	1.031	0.441	0.384
3	Rocks	18.1±1.2	27.7±1.6	142.11±4.6	200.903	1.447	0.648	0.543
4	Putty	15.4±0.8	3.8±0.6	35.3±4.1	23.56	0.164	0.105	0.636
5	Tile 1	31.6±1.1	78.8±2.6	274±9	187.882	1.336	0.614	0.507
6	Cement 2	39.3±1.2	66.9±2.4	356.9±10.8	162.448	1.168	0.544	0.438
7	Sand	31.6±0.9	58.4±1.8	508±11	154.228	1.133	0.502	0.416
8	Plaster of Paris	6.5±0.6	1.8±0.5	52.8±4.6	13.139	0.096	0.0531	0.035
9	White marble	4.5±0.4	0.6±0.3	6.5±1.5	5.858	0.0403	0.0279	0.016
10	Safedi	15.9±1.1	<0.1	<1.4	16.151	0.108	0.086	0.043
11	Samosam	26.8±1.0	<0.1	9.4±3.3	<25.167	0.169	0.134	0.068
12	Cement 1	41.6±1.2	60.6±2.2	317±10	152.667	1.094	0.525	0.412
13	Limestone	9.2±0.7	6.9±0.9	<1.4	<19.174	0.131	0.0766	0.051
14	White cement	26.8±0.9	16.4±1.1	74.8±5.2	56.012	0.392	0.223	0.152
15	Gypsum	20.8±0.8	31.8±1.5	394±11	96.612	0.719	0.317	0.261
12	Cement 1	41.6±1.2	60.6±2.2	317±10	152.667	1.094	0.525	0.412
13	Limestone	9.2±0.7	6.9±0.9	<1.4	<19.174	0.131	0.0766	0.051
14	White cement	26.8±0.9	16.4±1.1	74.8±5.2	56.012	0.392	0.223	0.152
15	Gypsum	20.8±0.8	31.8±1.5	394±11	96.612	0.719	0.317	0.261

3.1 Radium Equivalent Activity (Ra_{ea})

Ra_{ea} may be computed from the relation given below[23]:

$Ra_{ea} = 1.43A_c(Th) + A_c(Ra) + 0.077A_c(K)$

where $A_c(Th)$ is the activity concentration of ^{232}Th in $Bq.kg^{-1}$, $A_c(Ra)$ is the activity concentration of ^{226}Ra in $Bq.kg^{-1}$, $A_c(K)$ is the activity concentration of ^{40}K in $Bq.kg^{-1}$.

3.2 Internal Hazard Index (Hi_{nt})

The internal exposure to radon and its progeny is assessed by H_{int}, which is defined by the following relation:

$$H_{int} = (A_c(Ra)/185)+(A_c(Th)/259)+ (A_c(K)/4810)$$

3.3External Hazard Index (H_{ext})

The H_{ext} is interpreted as follows

$$H_{ext} = (A_c(Ra)/370) + (A_c(Th)/259) + (A_c(K)/4810)$$

3.4Exhalation Rate

Table 2 lists the J_{rm} in $mBq.kg^{-1}.h^{-1}$ and J_{ts} in $Bq.m^{-2}.h^{-1}$ for different samples. The J_{rm} varied from 4.5 to 21.55 $mBq.kg^{-1}.h^{-1}$ while J_{ts} extends from 42.44 to 2376.91 $Bq.m^{-2}.h^{-1}$. The average values were 11.287 $mBq.kg^{-1}.h^{-1}$ and 1128.246 $Bq.m^{-2}.h^{-1}$ for mass exhalation and surface exhalation rates, respectively. The distribution of radon and thoron exhalation rates in shown by graph given in Fig. 2 & 3. The highest value of J_{rm} and J_{ts} was observed for tile 2. The minimum value of J_{rm} for the white marble sample, while the lowest area exhalation rate was found for safedi. Fig. 4 shows the correlation (R^2=0.85) between ^{232}Th and ^{220}Rn surface exhalation rate, and Fig. 5 shows the correlation (R^2=0.81) plot between

Table 2 — J_{rm} and J_{ts} for the samples

Sr. No.	Sample Name	J_{rm} ($mBqkg^{-1}h^{-1}$)	J_{ts} ($Bqm^{-2}h^{-1}$)
1.	Rocks	10.5	1736.91
2.	Cement 1	11.27	421.12
3.	Cement 2	10.89	341.66
4.	White cement	21.55	1183.35
5.	Gypsum	7.55	262.55
6.	White Marble	4.5	925.71
7.	Limestone	5.91	125.12
8.	Putty	4.2	1078.12
9.	Tile 1	9.03	1691.16
10.	Samosam	6.5	612.3
11.	Plaster of Paris	4.8	498.13
12.	Tile 2	15.77	2376.91
13.	Tile 3	4.71	142.55
14.	Safedi	5.53	42.44
15.	Sand	8.87	93.66

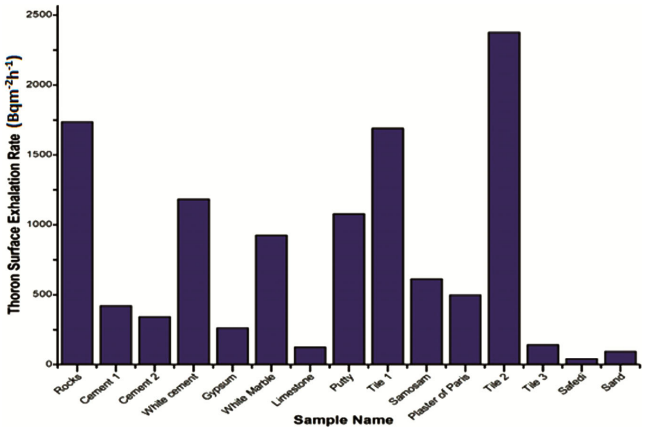

Fig. 2 — Bar distribution of thoron surface exhalation rate (J_{ts}) with samples.

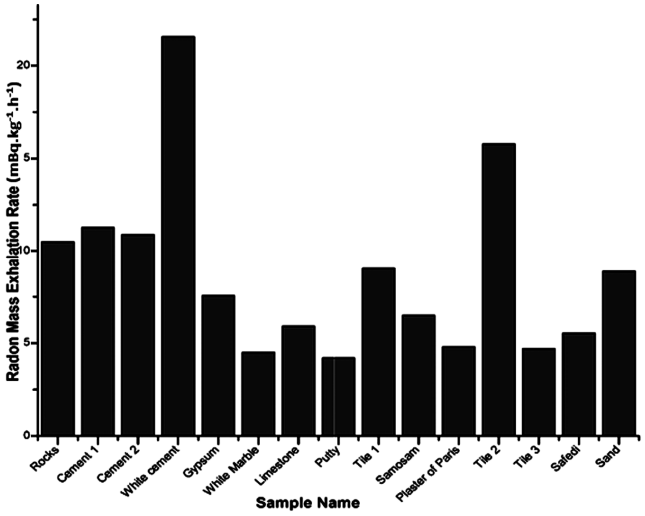

Fig. 3 — Bar distribution of radon mass exhalation rate (J_{rm}) with samples

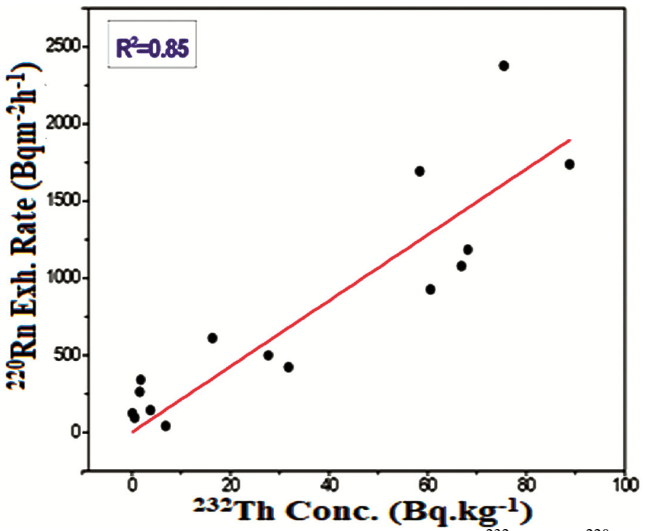

Fig. 4 — Correlation plot between the activity of ^{232}Th and ^{220}Rn exhalation

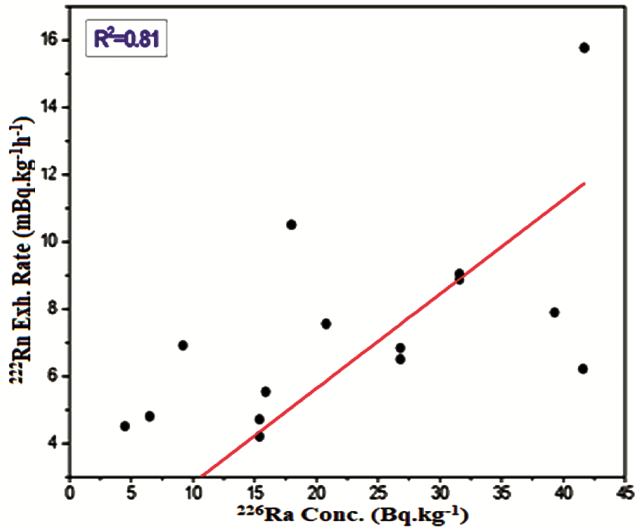

Fig. 5 — Correlation plot between the activity of ^{226}Ra and ^{222}Rn exhalation Rate

the activity of ^{226}Ra and ^{222}Rn mass exhalation rate of the samples. J_{rm} in the present study is below the worldwide average (57. 6 $Bqm^{-2}h^{-1}$). Hence residents do not possess any health hazards.

4 Conclusions

In this study, the activity of ^{226}Ra, ^{232}Th and K^{40} gamma spectrometry techniques using high resolution in some NORMS and TENORMS were measured by HPGe gamma spectrometer. Smart RnDuo monitor was used to measure the J_{rm} and J_{ts}. The correlations between the exhalation rates of these gases and their parent nuclide concentrations (radium/thorium) were examined. Finally, Ra_{ea}, I, H_{int} and H_{ext} were calculated. For ^{220}Rn, the J_{ts} ranged from 42.44 to 2376.91 $Bqm^{-2}h^{-1,}$ as shown in Fig. 2. In the case of ^{222}Rn, the J_{rm} varied from 4.5 to 21.55mBq kg^{-1} h^{-1}shown in Fig. 3**.** The activity of ^{226}Ra was found to vary between 4.5±0.4 Bq. kg^{-1} and 41.7±1.1 Bq. kg^{-1}. The activity of ^{232}Thwas found to be lies between 89.75 Bq. kg^{-1} and 0.1 Bq. kg^{-1}. The activity of ^{40}K was higher in the sand (508±11 Bq. kg^{-1}) and minimum in limestone(<1.4 Bq.kg^{-1}). The radiological parameters Ra_{ea} and H_{ext} were also within the recommended limits. The activity values attained from the current study show that the natural background radiations are in resemblance with other studies.

Acknowledgements

The authors, Deep Shikha and Vimal Mehta, want to acknowledge the funding received under the BRNS-DAE project (No. 56/14/01/2019-BRNS). The authors also want to acknowledge DBT- Star College Status Scheme (No. HRD-11012/4/2022-HRD-DBT).

References

1 Gammouh O S, Al-Smadi A M, Tawalbeh L I & Khoury L S, *Prev Chronic Dis*, 12 (2015).
2 Hamidalddin S H Q, *Int J Curr Microbiol Appl Sci*, 3(2014) 623.
3 Kaur R, Shikha D, Kaushal A,Gupta R, Singh SP, Chauhan RP & Mehta V, *J Radioanal Nucl Chem*, 330 (2021).
4 Efremova M & Izosimova A, *J Sustain Agricul*, 35 (2012) 250.
5 Jibiri N N, Farai I P & Alaus S K, *Radiat Environ Biophys*, 46 (2007) 53.
6 Vogeltanz-Holm N & Schwartz G G, *J Environ Radioact*, 192 (2018) 26.
7 Kaur R, Singh S P, Shikha D & Mehta V, *AIP Conf Proce*, 2357 (2022).
8 UNSCEAR, Effects of Ionizing Radiation,United Nations Scientific Committee on the Effects of Atomic Radiation, United Nations, 1 (2006).
9 WHO, World health statistics, World Health Organization, (2009).
10 Masahiro, Fujimoto K, Kobayashi S & Yonehara J, *Health Phys*, 66 (1994) 43.
11 Milic G, Jakupi B, Tokonami S, Trajkovic R, Ishikawa T, Celikovic I, Ujic P, Cuknic O, Yarmoshenko I, Kosanovic K & Adrovic F, *Radiat Meas*, 45 (2011) 118.
12 Kaur R, Shikha D, Mehta V & Singh S P, *Nucl Tech Radiat Prot*, 35 (2020) 268.
13 Mehta V, Shikha D, Singh S P, Chauhan R P & Mudahar G S, *Nucl Tech Radiat Prot*, 31 (2016) 299.
14 Semwal P, Singh K, Agarwal T K, Joshi M, Pant P, Kandari T & Ramola R C, *Acta Geophysica*, 66 (2018) 1203.
15 Rani S, Kansal S, Singla A K, Nazir S & Mehra R, *J Radioanal Nucl Chem*, 331 (2022) 1889.
16 Kansal S & Mehra R, *Int J Low Radiat*, 10 (2015) 1.
17 Shikha D, Kaur R, Gupta R, Kaur J, Sapra B K, Singh S P & Mehta V, *J Radioanal Nucl Chem*, 330 (2021) 1365.
18 Kumbakarni S, *Geological Survey of India Northern Region,* (Scientific agency, India), 2012.
19 Sapra B K, Mishra R, Sahoo B K, Rour R D, Kanse S D, Agarwal T K, Prajith R, Gaware J J, Jalauddin S & Kumbhar D H, *Appl Radiat Isot*, 60 (2004) 49.
20 Singh B, Kant K, Garg M & Sahoo B K, J Radioanal Nucl Chem, 326 (2020) 831.
21 Kaur S & Mehra R, Environ Geochem Health, 44 (2022) 1.
22 Kaur M, Kumar A, Mehra R & Mishra R, *Human Ecol Risk Assess*, (2018).
23 UNSCEAR, Effects and Risks of Ionizing Radiation, United Nations Scientific Committee on the Effects of Atomic Radiation, United Nations, 2 (2016).